

Segment-wise Description of the Dynamics of Traffic Congestion

T.S. Choi and K.Y. Michael Wong

Department of Physics, Hong Kong University of Science and Technology, Hong Kong

Kiwing To

Institute of Physics, Academia Sinica, Taipei

(Dated: August 7, 2018)

We compare the point-wise and segment-wise descriptions of the traffic system. Using real data from the Taiwan highway system with a tremendous volume of segment-wise data, we find that the segment-wise description is much more informative of the evolution of the system during congestion. Congestion is characterized by a loopy trajectory in the fundamental diagram. By considering the area enclosed by the loop, we find that there are two types of congestion dynamics -- moderate flow and serious congestion. They are different in terms of whether the area enclosed vanishes. Data extracted from the time delays of individual vehicles show that the area enclosed is a measure of the economic loss due to congestion. The use of the loss area in helping to understand various road characteristics is also explored.

I. INTRODUCTION

With the rapid development all over the world in the past few centuries, there is a huge demand for logistics or long distance transportation through the highway system. According to statistics from the Environmental Protection Administration Executive Yuan in Taiwan, the number of registered vehicles increased from 6.8 million in 2010 to 7.9 million in 2017. In Hong Kong, the number of registered vehicles is also rising continuously, from 0.57 million in 2008 to 0.77 million in 2018. This rising demand cannot be satisfied by the construction of new highways. Congestion is inevitably more frequent and more serious. Journeys of drivers are delayed whenever rush hours come. The increase of traveling time indicates an economic loss to the society. It is important to understand congestion so as to minimize the loss. Research was conducted on modelling and data analysis, in order to prevent the traffic system from entering the congestion phase [1, 4, 37]. However, the dynamics during congestion is not well-studied and still under debate [17, 19, 31, 32].

Conventional traffic models use observables at a point to describe the traffic condition [18, 21, 23]. For instance, if the speed detected is low, the traffic is considered to be congested. However, since stop-and-go waves exist in the traffic system during congestion, the speed at a point would fluctuate rapidly. The point-wise description is not capable of determining the traffic condition in this case. This problem can be solved by using a segment-wise description, as will be verified through simulations in this paper.

This study is based on real data from the Taiwan highway system. The data collection system was set up for the purpose of toll collection. Hence the data consists of the time information of individual vehicles passing through the sensors along their highway journeys. Highway segments can then be demarcated by successive sensors, enabling us to extract a tremendous volume of segment-wise information.

With the more precise segment-wise description of traffic congestions, we are able to trace the evolution of the traffic system during congestion, obtaining much clearer trajectories in the graph of flux versus density, which is also known as the fundamental diagram of traffic. We find that there are two different dynamics during congestion, the moderate flow and the serious congestion. They can be distinguished by the area enclosed by their trajectories in the fundamental diagram.

There is a further advantage of the individualized vehicle data from the toll collection system. In the past, the traffic data was mainly flux and averaged speed recorded at a point [18, 34]. The information of vehicle identity was missing. The delay suffered by a vehicle across two points on highway could not be measured. From the individual trajectory data from the toll collection system, we can compute the delay suffered by each vehicle, and hence deduce the economic loss incurred during a congestion event. We also show that the area enclosed in the fundamental diagram during congestion reflects the economic loss incurred.

The article is organized as follows. In Sec. II, we briefly discuss the conventional models in traffic theory and the debates of behaviors in congestion. We then introduce the point-wise and segment-wise descriptions. We illustrate the insufficiency of the point-wise description through the simulations of the optimal velocity model, and how it was outperformed by the segment-wise description. In Sec. III, behaviors of real traffic during congestion under the segment-wise description are reported. The concept of area in the fundamental diagram is also introduced, which facilitates the classification of dynamics during congestion. We show how the incurred economic loss is related to the macroscopic variables in the segment-wise description in Sec. IV. Finally, we summarize and discuss the implications of the area enclosed and various dynamics in congestion.

II. DESCRIPTIONS OF TRAFFIC SYSTEM

A. Conventional Traffic Models

The importance of studying highway traffic has long been recognized. The famous LWR model about traffic on highway was proposed around 1955 by Lighthill, Whitham and Richards [21, 30]. It was the most well-known model of traffic. The fundamental assumption of the model is that flux Φ and density ρ can be defined at any point on the highway, and the flux Φ is a function of the density ρ . The fundamental relation of traffic flow was defined as

$$\Phi = v\rho, \quad (1)$$

where v is interpreted as the average speed of the flow. Numerous works were developed afterwards [3, 24, 26, 36].

There are two phases of traffic systems in the model, the free flow phase, and the congestion phase according to the density of vehicles, ρ . There is a critical value of density, ρ_c . When $\rho < \rho_c$, the system is in the free flow phase. The flow speed v is a constant, corresponding to a free-will speed of vehicles, $v = v_{\text{free}}$. The flux Φ increases linearly with ρ . For $\rho \geq \rho_c$, the system is in the congestion phase. The interaction between vehicles becomes significant. The flow speed v is a decreasing function of ρ . The flux Φ decreases with ρ .

If vehicles are perfectly coordinated, they could maintain at almost the free-will speed independent of ρ . The decrease of v implies an increase of traveling time, and hence an economic loss to the society.

In the LWR model, these phases are defined in the steady state, in which the speed is steady and uniform for all vehicles. In reality, the traffic system is not in the steady state because of fluctuations of driver behaviors and vehicle influx.

However, there are situations that require a non-local description of the traffic. One situation arises in studying the impact of congestion to the society. The economic loss due to congestion is proportional to the total delay incurred during congestion. In the point-wise description, the delay can only be approximated from the decrease in speed. However, as congestion is a phenomenon with finite length, this approximation requires a frequent sampling of points on the highway to be accurate. On the contrary, in the segment-wise description, the total delay comes naturally as it is just the increase in traveling time along the segment. We shall show that it is possible to compute the economic loss through macroscopic variables in the segment-wise description.

Another situation arises in clarifying the nature of congestion proposed by various traffic theories. For example, with observations from real congested traffic patterns, Kerner proposed the notion of synchronized flow [13–15, 18–20]. In this notion, the conventional congestion phase is composed of two other phases, “the syn-

chronized flow” and “the wide moving jam”. The two behaviors mainly differ in the property at the downstream front. The “wide moving jam” traffic phase is defined as a moving jam with a propagating constant-speed downstream front [16]. The “synchronized flow” phase is defined as a complement of the “wide moving jam” traffic phase. The location of the downstream front in the synchronized flow is fixed but the mean velocity of vehicles in the downstream front is not maintained during the phase. Although there are already lots of works modeling this three phase traffic theory [5, 7, 10, 11], there were criticisms of its inconsistency in the definition of the synchronized phase [32]. It was suggested that the synchronization of vehicle speed among different lanes was merely a transient characteristic of the “synchronized flow” at the beginning of the three-phase traffic theory [18], but it was found later by Kerner that this behavior could be observed in congestion [16].

These discussions bring up the need of a segment-wise description in analyzing congestion. It is noted that the two phases introduced by Kerner require knowledge of behaviors at the downstream front, and could not be recognized by examining the density and flux at a point only. In the conventional LWR model, the fundamental relation, Eq. (1), is only defined at a point, and hence is just a point-wise description of the traffic system. While settling these controversies is not the intention of this article, it is essential that the ultimate solution requires a segment-wise description. On the other hand, this article focuses more on the dynamical picture of congestion and identify two different system behaviors.

B. The 1-point Measure and the 2-point Measure

There are various ways to describe a traffic system. They are mainly different in definitions of the major observables: density ρ , flux Φ , and speed v .

A point-wise description uses information at a fixed location on the system [18, 21, 29]. Consider a detector placed at a fixed point x on the highway, and a vehicle passing through the detector. The information collected would be a time interval $[t_1, t_2]$ when the vehicle is on the detector. Hence, the vehicle would contribute to the flux at time t_1 . Its speed can be approximated as

$$v_i = \frac{L_{\text{veh}}}{|t_2 - t_1|}, \quad (2)$$

where L_{veh} is the typical length of a vehicle. There is no information of the density ρ but it can be computed through the Edie’s definition [6]. For an observation time interval $[t, t + \Delta t]$. The flux is

$$\Phi_1(x, t) = \frac{n(x, t)}{\Delta t}, \quad (3)$$

where $n(x, t)$ is the number of vehicles passing through x in $[t, t + \Delta t]$. The density follows from the fundamental

relation, Eq. (1) with the harmonic mean of speed [6]

$$\rho_1(x, t) = \frac{\Phi_1(x, t)}{v_{\text{har}}(x, t)}, \quad (4)$$

$$v_{\text{har}} = \left(\frac{1}{n(x, t)} \sum_{i=1}^{n(x, t)} \frac{1}{v_i} \right)^{-1}. \quad (5)$$

A large number of studies employed this definition of (ρ_1, Φ) [9, 12, 17–19, 25, 34]. However, v_{har} would be greatly affected by low speed vehicles, and hence fluctuates rapidly in congestion. The computed density ρ_1 might be affected. The formula may work well when the system is steady and uniform. In the case of large fluctuations in speed, ρ_1 may not reflect the true condition of the system.

A segment-wise description uses information of vehicles within a segment. A commonly accepted segment-wise definition of Φ and ρ is stated in the Highway Capacity Manual [27, 35]. Consider a road segment $[x - L, x]$ on the highway and an observation time interval $[t, t + \Delta t]$. The flux Φ_2 is defined to be the number of vehicles passing the downstream end x within the time interval, while the density ρ_2 is defined as the averaged number of vehicles along the road segment at time t . From the definition, Φ_2 is the same as that in the point-wise description,

$$\Phi_2(x, t) = \frac{n(x, t)}{\Delta t}. \quad (6)$$

The density ρ_2 is different,

$$\rho_2(x, t) = \frac{\alpha(x, t)}{L}, \quad (7)$$

where $\alpha(x, t)$ is the number of vehicles in $[x - L, x]$ at a time t .

It is worth mentioning that $\rho_2 L = \alpha$ is the total number of vehicles in the segment. Through describing the traffic system in this way, we are making an analogy with the queuing theory. The flux in traffic system corresponds to the service rate in the queuing theory [2]. With more vehicles accumulated on the segment, the time to pass through the segment increases.

In fact, the quantity α is the accumulation introduced by Daganzo [4, 8]. Accumulation is the number of vehicles in the traffic system. It is a convenient quantity as it is additive when two or more segments are combined. A macroscopic fundamental diagram was successfully reproduced by summing different links on the traffic network in an area.

The accumulation α can be obtained by taking a snapshot of the system and counting the number at any given time. It is difficult and demanding in real practice. Instead, it can be obtained easily through monitoring detectors at the upstream and downstream ends.

For a closed road segment, by conservation of flow, the time evolution of α follows the equation

$$\alpha(t) = \alpha(t_0) + \int_{t_0}^t (\Phi(x - L, t') - \Phi(x, t')) dt', \quad (8)$$

with $\Phi(x - L, t')$ and $\Phi(x, t')$ denoting the flux detected at the upstream and downstream ends, respectively, and $\alpha(t_0)$ denoting the number of vehicles in the system initially. It would be negligible by starting the computation of α when $\alpha(t_0)$ is close to 0 by common sense, such as 3:00 a.m.

Hence, the definition of (ρ_2, Φ) requires information from two locations, $(x - L)$ and x .

To emphasize the difference between the two descriptions, they are hereafter named as the 1-point measure and the 2-point measure, respectively. The 1-point measure uses the information of appearance and speed at the downstream end, while the 2-point measure uses the information of appearance at the upstream end and the downstream end.

C. Comparison in Simulations

The two descriptions are equivalent when the system is steady and uniform. Suppose N vehicles move with speed v and span the system evenly. Then the average number of vehicles per length is just $\frac{\alpha}{L}$ from the 2-point measure. The number of vehicles in the region $[x - \Delta x, x]$ is $\frac{\alpha}{L} \Delta x$. Then for a time interval Δt , the number of vehicles passing x is the number of vehicles within the region $[x - v\Delta t, x]$,

$$n = \frac{\alpha}{L} v \Delta t. \quad (9)$$

Hence, from Eq. (4),

$$\rho_1 = \frac{n}{v \Delta t} = \frac{\alpha}{L} = \rho_2. \quad (10)$$

This steady and uniform condition holds in the free flow phase, but not in the congestion phase.

We compare the two descriptions through simulations of the optimal velocity model (OVM). The purpose of doing these simulations is that we can control the parameters in simulations and hence fix whether the system is in the free flow phase or in the congestion phase.

The OVM is well-studied in various literature [28, 29, 33]. It is a single lane model. Every vehicle has an optimal velocity to achieve. This optimal velocity $V(h(t))$ depends on the headway distance $h(t)$ only and is homogeneous among vehicles. The headway distance h is defined as the distance between the center of mass of vehicle with that of the one ahead. There are two contributions to the acceleration. One is the relaxation of the current speed v to $V(h)$. The other one depends on the velocity of the vehicle ahead as seen by the driver. Drivers tend to follow the speed of the vehicle ahead.

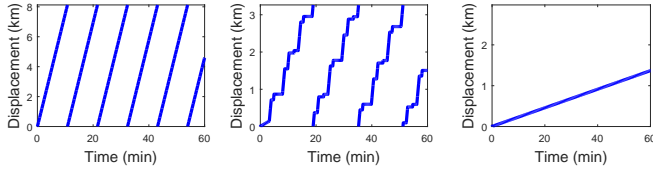


Figure 1. Trajectories of a vehicle from OVM with $N = 250$, in free flow phase $L_{\text{sim}} = 8.13$ km (left), intermediate phase $L_{\text{sim}} = 3.26$ km (middle), slowly moving jam phase $L_{\text{sim}} = 2.98$ km (right). The range of y-axis is the same as L_{sim} .

The OVM can be summarized by the following sets of differential equations,

$$\begin{cases} \dot{h}_i(t) = v_{i+1}(t) - v_i(t) \\ \dot{v}_i(t) = \frac{1}{T} (V(h_i(t-\tau)) - v_i(t-\kappa)) + \beta \dot{h}_i(t-\sigma) \\ V(h) = v_{\max} \begin{cases} 0 & \text{if } h < L_{\text{veh}} \\ \frac{(h-L_{\text{veh}})^3}{8L_{\text{veh}}^3 + (h-L_{\text{veh}})^3} & \text{if } h \geq L_{\text{veh}} \end{cases} \end{cases}, \quad (11)$$

where $L_{\text{veh}} = 7.5$ m is the typical length of vehicles [23], $v_{\max} = 110$ kmh $^{-1}$. τ , κ and σ models the reaction times of driver to the observables h_i , v_i , \dot{h}_i , respectively. T and β are which can be determined by the following.

Drivers have different reaction times on different quantities in general. We employ the human driver set-up. Drivers take time to respond to the change in relative position, but they could react instantaneously to self motion. The parameters are then set to be $\tau = \sigma = \frac{2L_{\text{veh}}}{v_{\max}} = 0.4904$ s, $\kappa = 0$. $T = \frac{2L_{\text{veh}}}{v_{\max}} = 0.4904$ s, $\beta = \frac{v_{\max}}{10L_{\text{veh}}} = 0.407$ s $^{-1}$ [29].

We simulate the model on a system of length L_{sim} , with periodic boundary condition. Random sequential update is applied. Vehicles are distributed uniformly on the segment with random initial speeds. By varying L_{sim} , the system evolves from the free flow phase to the congestion phase.

Figure 1 shows the trajectories of one vehicle in different situations. When L_{sim} is large, the system is in the free flow phase. Vehicles do not interact with each other. The trajectories are straight and their speeds are steady. When L_{sim} decreases to the intermediate regime ($L_{\text{sim}} = 3.05$ km), vehicles are forced to interact. A vehicle stops if it is too close to the vehicle ahead, and accelerates when there is free space. This results in winkles on the trajectories. The phenomenon is usually referred to as a stop-and-go wave in the literature. The system is in the congestion phase as it is not in the free flow phase anymore. When L_{sim} continues to decrease, vehicles become too close to each other. All vehicles could not accelerate too much and are synchronized. The trajectory is a straight line without winkles. Vehicles move together at a steady and extremely low speed.

To compare the 1-point measure and 2-point measure, we consider a subsystem of the whole simulation environment. Let there be two detectors collecting information of passing vehicles at x_1 and x_2 , with $x_2 > x_1$. Vehicles

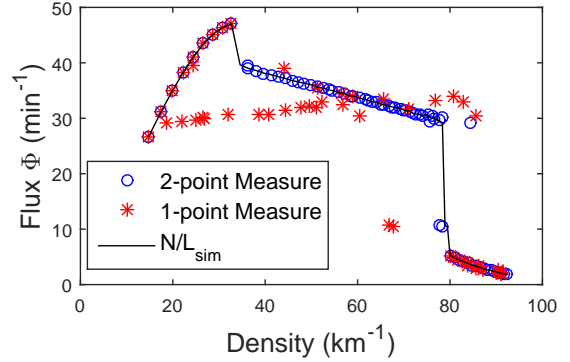


Figure 2. Fundamental diagram from 1-point measure (red star) and 2-point measure (blue circle) of the optimal velocity model by varying segment length $L_{\text{sim}} \gg 1$ km, with $\Delta t = 1$ min, $\|x_2 - x_1\| = 0.08L_{\text{sim}}$. Each point is an average over the time series after transient. $\left\{ \frac{N}{L_{\text{sim}}}, \Phi \right\}$ is plotted in black line as a reference. Vehicles are initially distributed evenly on the road segment, with normalized initial speed v following a normal distribution, $\frac{v}{v_{\max}} \sim N\left(\frac{1}{2}, \frac{1}{6}\right)$.

are considered to be traveling from x_1 to x_2 . The 1-point measure uses the appearance and speed of vehicles from the detector at x_2 only, while the 2-point measure uses the appearance of vehicles at x_1 and x_2 . The flux going out of the subsystem $[x_1, x_2]$ is the rate of vehicles detected at x_2 .

Figure 2 shows the fundamental diagram generated from major observables of the two descriptions. We also plot $\left\{ \frac{N}{L_{\text{sim}}}, \Phi(x_2) \right\}$ on the fundamental diagram. Since N and L_{sim} are parameters that control the behaviors of the model, $\frac{N}{L_{\text{sim}}}$ could be treated as a reference density of the system. The two descriptions coincide with the reference value when L_{sim} is either too large or too small. The 1-point measure deviates from the reference line for intermediate L_{sim} . This is expected since the steady and uniform conditions do not hold for intermediate L_{sim} . The computation of density ρ_1 depends on the speed of vehicles at x_2 , from Eq. (4). As shown in the trajectory in Fig. 1, the speed fluctuates in between two extremes, fast or stationary. When the winkles are upstream of the detector, only fast vehicles passing the detector contribute to the computation of ρ_1 . The density would be underestimated. On the other hand, when the winkles are on the detector, only slow vehicles contribute. It results in an overestimation of the density. Depending on the time at which a winkle is on the detector, ρ_1 would deviate from the reference value in different ways. This shows that the 1-point measure is not robust to congestion behaviors. In contrast, ρ_2 is robust to this fluctuation of vehicle speed, and coincides with the reference line. It is noted that the result is independent of the length of the subsystem, unless it is too small.

The purpose of a fundamental diagram is to determine the phase of a traffic system. A system is said to be

congested when $\rho > \rho_c$. Due to speed fluctuations, for a system in the intermediate regime, the local density ρ_1 estimated from the 1-point measure could be smaller than the critical value, $\rho_1 < \rho_c$. It fails to indicate what phase the system is currently at.

From this simple simulation of the optimal velocity model, we show that there is a difference in point-wise description and segment-wise description, after the breakdown of the free flow phase. The 2-point measure is robust to speed fluctuations in congestion and matches the reference density. This shows that in studying congestion, it would be more reliable by employing the segment-wise 2-point measure.

III. CONGESTION IN REALITY

We analyze real data from the Taiwan highway system, which consists of 10 national highways and numerous provincial highways. There are 2 major highways connecting the northern and southern parts of Taiwan, with a length of about 400 km, respectively. In 2006, the Electronic Toll Collection system replaced the traditional toll stations. Overhead detectors were installed on major highways. Whenever a vehicle passes under these detectors, its identity, location and time of appearance would be recorded. This provides a precious opportunity in studying real traffic systems.

The analysis is performed by applying the 2-point measure. Since velocity data is not available from the dataset, the 1-point measure is not applicable. Nevertheless, as demonstrated in the OVM simulation in the next section, the characterization of congestion using the loop area enclosed in the fundamental diagram is much more obscured if 1-point measurements are adopted. The density of a segment in between any two consecutive detectors is computed by Eq. (8). There are entrances from the local streets and exits to the local streets in the segments. We approximate the locations of highway entrance and exit in a segment to be the locations of the downstream and upstream ends, respectively. It corresponds to the location of the first and last detections of the entering or exiting vehicles in the segment, respectively. As the number of vehicles entering or exiting the segment is small compared with the number of vehicles traveling across the segment, their contributions are negligible, and the approximation is reasonable.

Typically, a truncated fundamental diagram is observed through the 2-point measure for almost all the 300 segments in the Taiwan highway system. An example is shown in Fig. 3. When the density is small, the system is in the free flow phase. The flux rises linearly with the growth of density. The free flow phase breaks down for sufficiently large density as expected, typically at $\rho_2 \approx 50 \text{ km}^{-1}$. For the Taiwan highway system with 3 lanes typically, it is equivalent to a headway distance of about 60 m. It is roughly the displacement of a vehicle traveling at the speed limit of 110 kmh^{-1} for 2 s. This is

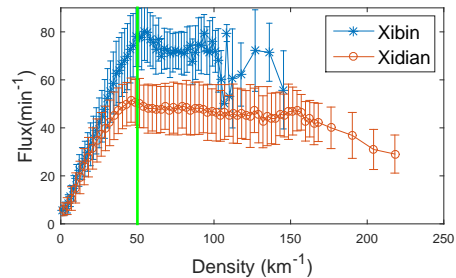


Figure 3. Flux Φ versus density $\rho_2 = \frac{\rho}{L}$ from Taiwan highway data, collected in February 2016, averaged over 29 days. Data collected in segment from Xibin to Zhunan (blue star) and from Xindian to Ankeng (red circle). The length L of the segments are 5.4 km and 3.6 km, respectively. The vertical green line indicates the line $\rho_2 = 50 \text{ km}^{-1}$.

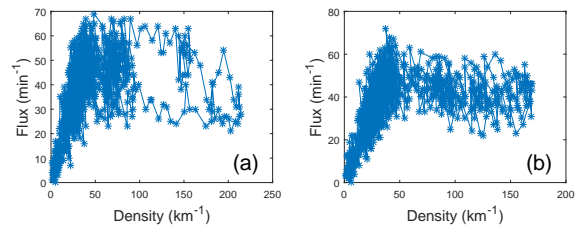


Figure 4. The daily dynamics of the system on the fundamental diagram. Data collected in the segment from Xindian to Ankeng, with a length of 3.6 km (a) on 7-Feb, 2016, and (b) on 24-Feb, 2016. Each data point is measured in one minute interval, from 5 : 00 a.m. to 11 : 00 p.m.

consistent with an experimental finding by McGehee in 2000 [22], which shows that the driving reaction time in crash avoidance is about 2.3 s on average.

The time-averaged congestion behavior agrees with the prediction of conventional theory. However, this assumes that the variation of flux at a given density is caused by random fluctuations only. It also neglects the time correlation in the data. To get better insights of how congestion unfolds, we consider the time dependence of the system state in the fundamental diagram. Figure 4 shows examples of daily evolution of the traffic system on the fundamental diagram. It can be observed that there are two types of evolution after the breakdown of the free flow phase. A loopy evolution can be observed in Fig. 4(a) while the flux in Fig. 4(b) remains at a high level around $40 - 50 \text{ min}^{-1}$.

To understand the physical picture of these dynamics, the time series of the flux at the upstream end (influx) and the downstream end (outflux) are investigated. The influx always leads the outflux in the free flow phase due to the finite time for vehicles to traverse the segment. However, this time correlation may not be maintained during congestion.

Figure 5 shows the flux evolution during congestion. For the loopy dynamics in Fig. 4(a), there was a sudden drop in outflux in Fig. 5(a) around 02 : 15 p.m. The out-

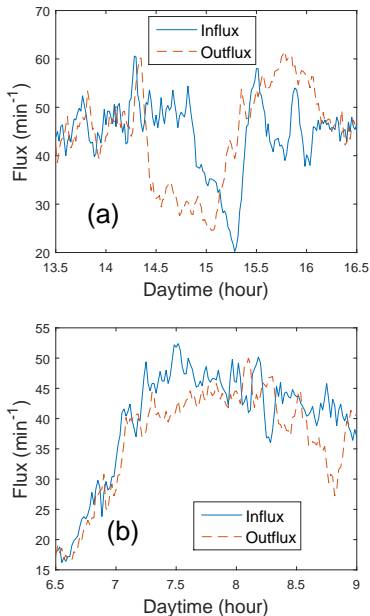


Figure 5. The time evolution of influx and outflux of the segment from Xindian to Ankeng, with a length of 3.6 km (a) on 7-Feb, 2016, and (b) on 24-Feb, 2016.

flux remained low while the number of vehicles inside the system built up. A significant drop of influx followed at around 03 : 00 p.m. The system recovered to the normal flux level when the density reached the maximum value of about 200 vehicles per km. It can be observed that the influx was slightly leading the outflux before 02 : 15 p.m. Afterwards, this relation was reversed. The outflux led the influx, indicating a possibility of back propagation of congestion.

This reverse of time correlation is not observed for the dynamics in Fig. 4(b). The correlation between influx and outflux was lost during congestion, starting from around 07 : 15 a.m. This may be explained by stochastic interactions among individuals. The interaction was internal among the vehicles and hence did not affect the influx.

This suggests that there are two possible dynamics after the breakdown of the free flow phase. To verify whether the two cases are qualitatively different, or merely correspond to loops of different sizes, we need to quantify these congestion behaviors. It is noted that they are common in having an increase in accumulation, and are different in whether there is a sharp drop in outflux. The product of these two factors approximates the area enclosed by the dynamics during congestion in the fundamental diagram. Therefore, it is natural to use the area enclosed to quantify these behaviors.

Suppose the system experiences a loopy dynamics during a time interval $[t_a, t_e]$, the area enclosed by the tra-

jectory can be computed by

$$A(t_a, t_e) = \oint \Phi_{\text{out}}(t) d\rho_2(t), \quad (12)$$

where the closed path integral is done along the trajectory of the dynamics in the fundamental diagram, with the two end points being connected. With assumptions on the behaviors at the end points $t = t_a, t_e$, and some approximations, it can be shown (in Appendix A) that

$$A(t_a, t_e) \approx \frac{|t_e - t_a|}{L} \times (\text{cov}_{[t_a, t_e]}(\Phi_{\text{in}}, \Phi_{\text{out}}) - \text{cov}_{[t_a, t_e]}(\Phi_{\text{out}}, \Phi_{\text{out}})), \quad (13)$$

where

$$\text{cov}_{[t_a, t_e]}(A, B) = \frac{1}{|t_e - t_a|} \times \int_{t_a}^{t_e} (A(t) - \bar{A}(t)) (B(t) - \bar{B}(t)) dt, \quad (14)$$

denotes the covariance of the two time series $A(t)$ and $B(t)$ in the time interval $[t_a, t_e]$.

As $\text{cov}_{[t_a, t_e]}(\Phi_{\text{out}}, \Phi_{\text{out}})$ is always positive, and an approximation of $\bar{\Phi}_{\text{in}} \approx \bar{\Phi}_{\text{out}}$,

$$\text{cov}_{[t_a, t_e]}(\Phi_{\text{in}}, \Phi_{\text{out}}) \leq \text{cov}_{[t_a, t_e]}(\Phi_{\text{out}}, \Phi_{\text{out}}). \quad (15)$$

Hence, $A(t_a, t_e) < 0$. The sign of the area enclosed $A(t_a, t_e)$ indicates the orientation of the loop. This matches the physical picture as described in Fig. 4(a). The loops are typically anticlockwise, starting with a sudden drop of flux and then an increase of accumulation.

To investigate whether there are really two types of dynamics, we analyze data from a large number of segments in Taiwan. To employ Eq. (12), the time interval $[t_a, t_e]$ needs to be defined. As we are investigating the dynamics after the breakdown of free flows, there is a natural threshold $\alpha_c = L \times 50 \text{ km}^{-1}$ as the breakdown accumulation. For a time interval $[t_a, t_e]$ to be identified as the congestion time interval, it must satisfy the following criteria: (1) $\forall t \in (t_a, t_e), \alpha(t) > \alpha_c$; (2) $\alpha(t_a), \alpha(t_e) \leq \alpha_c$. An example of the time intervals identified by the criteria is shown in Fig. 6.

In addition to the area enclosed in $[t_a, t_e]$, the range of drop of the outflux in $[t_a, t_e]$, $\Delta\Phi(t_a, t_e)$ is also recorded. It is defined as

$$\Delta\Phi(t_a, t_e) = \max_{t \in [t_a, t_e]} (\Phi_{\text{out}}(t)) - \min_{t \in [t_a, t_e]} (\Phi_{\text{out}}(t)). \quad (16)$$

Figure 7 shows how the area enclosed $A(t_a, t_e)$ depends on the range of outflux drop in different segments. When the drop is small, the area enclosed is also small. We may classify this dynamics as the one illustrated in Fig. 4(b). When the drop of the outflux exceeds a threshold, $A(t_a, t_e)$ increases sharply. This indicates the occurrence of loopy dynamics. The threshold for the onset of loopy dynamics varies for different segments, which may depend on individual characteristics. The drastic increase

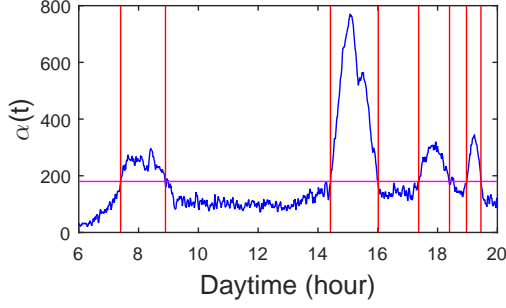


Figure 6. Illustration of congested time intervals $[t_a, t_e]$ (indicated by the pairs of red lines), selected by the criteria: (1) $\forall t \in (t_a, t_e), \alpha(t) > \alpha_c$; (2) $\alpha(t_a), \alpha(t_e) \leq \alpha_c$. The purple line indicates the threshold, $y = \alpha_c$. Data collected from the system, Xindian to Ankeng, on 16-Feb, 2016 with a length $L = 3.6$ km.

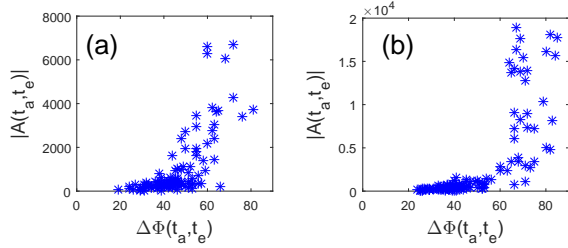


Figure 7. The area enclosed in the congestion $A(t_a, t_e)$ versus the drop of the outflux in the congestion $\Delta\Phi(t_a, t_e)$. Data collected from the system in Feb, 2016, (a) from Wugu to Sanchong with a length $L = 3.7$ km; (b) from Neili to Jongli with a length $L = 2.5$ km.

of $A(t_a, t_e)$ with respect to $\Delta\Phi(t_a, t_e)$ supports the existence of two dynamics after the breakdown of the free flow phase. We classify the dynamics in Figs. 4(a) and (b) as “serious congestion” and “moderate flow”, respectively.

IV. ECONOMIC LOSS INCURRED IN CONGESTION

A. Economic Loss in Reality

Whenever there is congestion, there is an increase of traveling time across the system. From drivers’ point of view, there is always a better way to spend this delay than suffering from congestion. From society’s point of view, wasting time on transportation does not produce any value to the economy of the society. Hence, the total incurred delay can be used to represent the economic loss during congestion.

The latency is defined as the traveling time across the system. Denote the minimum latency across the system as l_{free} . When a driver suffers from congestion, the latency increases from l_{free} to l . The monetary loss incurred

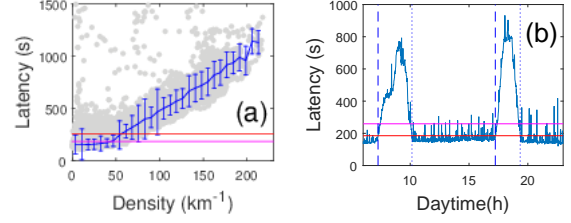


Figure 8. (a) Latency $l(t)$ versus the scaled accumulation $\frac{\alpha(t)}{L}$ on the same segment. The horizontal lines indicate the expected latency if a vehicle travel at 50 km/h (purple), and 70 km/h (red). (b) An example of the time evolution of $l(t)$. Data collected from the system on 24-Feb, 2016, from Xindian to Ankeng with a length $L = 3.6$ km. The vertical lines indicate the congestion time interval $[t_a, t_e]$ identified by the conditions. The dashed lines and the dotted lines mark the start and end of the time intervals, respectively.

on the society is $\beta(l - l_{\text{free}})$, where β is the value of time. It might vary among individuals, but for simplicity, it is set to be homogeneous and $\beta = 1$. The economic loss of the society E_{loss} is

$$E_{\text{loss}} = \sum_{i=1}^{N_{\text{tot}}} \beta_i (l_i - l_{\text{free}}) = \sum_{i=1}^{N_{\text{tot}}} (l_i - l_{\text{free}}), \quad (17)$$

where l_i is the latency of the i th driver, and N_{tot} is the number of vehicles being affected by congestion. N_{tot} can be computed by consideration of the influx in the congestion time interval,

$$N_{\text{tot}} = \int_{t_a}^{t_e} \Phi_{\text{in}}(t) dt. \quad (18)$$

Let $l(t)$ be the average latency of vehicles entering a segment at time t . The economic loss incurred by congestion in $[t_a, t_e]$ can be expressed in terms of Φ_{in} ,

$$E_{\text{loss}} = \int_{t_a}^{t_e} (l(t) - l_{\text{free}}) \Phi_{\text{in}}(t) dt. \quad (19)$$

To compute l_i or $l(t)$, the information of the entrance time and exit time of the i th individual is required. A tracking of vehicle’s identity across different detectors is needed. The conventional detectors on the highway only measure the number of vehicles passing through, without tracing the identity of vehicles. In contrast, the electronic toll collection system enables us to track the latency of individual vehicles.

The congestion time interval $[t_a, t_e]$ could also be defined using $l(t)$. The system is defined to be congested in a time interval $[t_a, t_e]$ if the following conditions hold. (1) $\|t_e - t_a\| > T$, for $T > 0$; (2) $\forall t \in (t_a, t_e), l(t) > l_{\text{ref}}$; (3) $l(t_a), l(t_e) < l_{\text{ref}}$; (4) $\exists t \in (t_a, t_e), l(t) > l_{\text{jam}}$. Condition (2) and (3) are equivalent to the conditions listed in Sec. III. Conditions (1) and (4) are added in consideration of the rapid fluctuations of the latency time series.

The parameters in these conditions are set in the following way. The parameter l_{ref} is the reference latency, determined by the average latency before breakdown as illustrated in Fig. 8(a). The parameter l_{jam} is set in order to filter out points in which the latency is large due to fluctuations,

$$l_{\text{jam}} = l_{\text{ref}} + \sigma_{l_{\text{ref}}}, \quad (20)$$

with $\sigma_{l_{\text{ref}}}$ being the standard deviation of $l(t)$ at the breakdown point. The time interval T is set to a sufficiently large value to identify a sustained congestion period despite rapid fluctuations of the latency $l(t)$.

Figure 8(b) shows an example of the identification of the congestion time interval through $l(t)$. In this example, the values of l_{ref} and l_{jam} correspond to the expected traveling time for a vehicle of speed 70 km/h and 50 km/h, respectively in Fig. 8(a), and T is set to be 10 min.

To compute E_{loss} , we note that the time saved by traveling beyond the speed limit should not be counted as a benefit to the society. Hence the time saved for traveling time shorter than l_{ref} is discarded in the following empirical formula for E_{loss} ,

$$E_{\text{loss}} = \int_{t_a}^{t_e} \max(l(t) - l_{\text{ref}}, 0) \Phi_{\text{in}}(t) dt. \quad (21)$$

The evolution of the loopy dynamics consists of the following stages. There is an initial drop of the outflux, followed by an increase in the density. When the system recovers, the outflux increases, followed by a decrease in the density back to the normal state. In reality, the transitions between these stages is not sharp, but by assuming sharp transitions the area becomes rectangular. Hence we are able to relate the economic loss E_{loss} and the area enclosed $A(t_a, t_e)$ (shown in Appendix B),

$$\frac{E_{\text{loss}}}{N_{\text{tot}}} \approx \frac{L}{2f\Phi_{\text{acc}}^2} A(t_a, t_e), \quad (22)$$

where the economic loss is scaled by N_{tot} , the total number of vehicles using the segment during the congestion period, and f is the fractional decrease of the flux during the congestion time interval. This fractional decrease reflects the decrease of highway capacity as part of the highway may be blocked. Φ_{acc} indicates the influx to the system when the loopy dynamics starts. Hereafter the area $A(t_a, t_e)$ will be referred to as the loss area.

Figure 9 shows how the economic loss per vehicles $\frac{E_{\text{loss}}}{N_{\text{tot}}}$ is related with the area enclosed $A(t_a, t_e)$. A clear linear relation can be observed. By a linear fitting,

$$\frac{E_{\text{loss}}}{N_{\text{tot}}} = mA(t_a, t_e) + c, \quad (23)$$

with $m = 4.47 \times 10^{-4} \text{ km}\cdot\text{min}^2$ and $c = 2.72 \text{ min}$. $c \neq 0$ because Eq. (22) apply for loopy dynamics only. From the criteria listed, E_{loss} must be non-zero. The intercept may correspond to the economic loss due to moderate

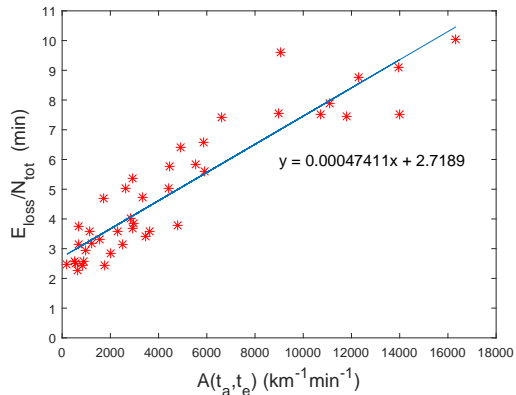


Figure 9. Economic loss per vehicles $E_{\text{loss}}/N_{\text{tot}}$ versus the area enclosed $A(t_a, t_e)$. Data collected on the segment from Xindian to Ankeng with a length $L = 3.6 \text{ km}$. The blue solid line is a linear fitting of the data, with slope $m = 4.47 \times 10^{-4} \text{ km}\cdot\text{min}^2$ and intercept $c = 2.72 \text{ min}$.

flows in Fig. 4(b), since their loss areas vanish. We can use the slope m to approximate Φ_{acc} averaged among different loopy dynamics by Eq. (22), $\langle \Phi_{\text{acc}} \rangle = \sqrt{\frac{L}{2fm}} = 72.7 \text{ min}^{-1}$ where $f \approx 0.7$ from real data, approximated by

$$f = \frac{\max_{t \in [t_a, t_e]} (\Phi_{\text{in}}(t)) - \min_{t \in [t_a, t_e]} (\Phi_{\text{out}}(t))}{\max_{t \in [t_a, t_e]} (\Phi_{\text{in}}(t))}. \quad (24)$$

Φ_{acc} has the same order of magnitude as the typical flux before breakdown of this segment, which is about 50 min^{-1} shown in Fig. 3. The deviation may arise from the approximation in the derivation of Eq. (22), where we have neglected the interactions between vehicles. For example, during an accident, vehicles traveling on the lane with obstacles ahead would try to switch to other lanes. This interaction between vehicles from different lanes would cause further delays.

Hence, the economic loss per vehicle is highly correlated with the area enclosed. We are able to determine the average delay suffered by the drivers during congestion from macroscopic information shown on the fundamental diagram.

This also suggests that the social impacts from the two congestion dynamics are different. For moderate flow with a smaller area enclosed, its impact is also small corresponding to the intercept in Fig. 9. For serious congestion, the average delay could be huge, growing with the area enclosed.

B. Economic Loss in Simulation

To further investigate the information hidden in the relation between the loss area and the economic loss,

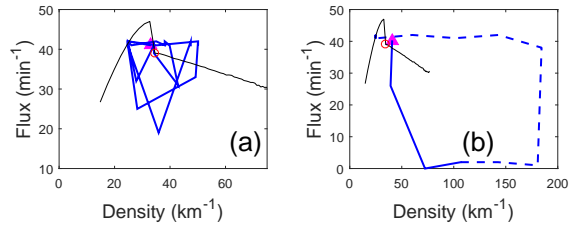


Figure 10. (a) Moderate flow and (b) serious congestion in the simulations. The blue lines indicate the evolutions of the system during the congestion. The black line is the reference line as shown in Fig. 2. The red circle indicates the state of the system in simulations. The serious congestion is observed in the accident condition with $\tau = 5$ min. The purple triangle indicates the starting point of the evolution. In Fig. 10(b), two linestyles are employed to illustrate the orientation of the evolution. The dashed line indicates the evolution of the system in the first 3 min after the accident, while the solid line is the evolution afterwards. In Fig. 10(a), only solid line is used for clarity. The graphs are drawn in different scale to have a better illustration of the difference between the dynamics.

we simulate the loopy dynamics by the optimal velocity model. In the simulation, we vary the location of the accident $x_{\text{acc}} = r \|x_2 - x_1\|$ from the upstream end, for $0 < r < 1$. A vehicle at position x_{acc} is forced to move with speed $v = 0.01v_{\text{max}}$ for a time τ . We control the scale of the accident by tuning τ . It can also be interpreted as the road clearing time of an accident in reality. The congestion time interval counts from the start of the control until the system recovers to the normal state.

The two dynamics classified in real traffic can also be found in the optimal velocity model. Figures 10(a) and (b) show the moderate flow and serious congestion in simulation, respectively. Without any accidents introduced, the flux remains constant with small density fluctuations. By introducing an accident to the system with $\tau = 5$ min, $r = 0.9$, the serious congestion with an anti-clockwise loopy dynamics is observed.

We compare the 2-point measure and the 1-point measure in describing the evolution during accidents with different τ . Figure 11(a) shows a significant increase of the loss area from the 2-point measure when τ increases. On the contrary, the area enclosed by trajectories from the 1-point measure is neither well defined nor correlated with τ . This shows the advantage of the 2-point measure in describing behavior in congestion.

Figure 12 illustrates how the relation between economic loss $\frac{E_{\text{loss}}}{N_{\text{eff}}}$ and the area enclosed $A(t_a, t_e)$ changes with different accident location $x = r \|x_2 - x_1\|$, and road clearing time τ . For large $r \geq 0.6$, $\frac{E_{\text{loss}}}{N_{\text{tot}}}$ increases linearly with $A(t_a, t_e)$. This is similar to the finding from real data.

Notice that the economic loss saturates in τ for large r , i.e., the economic loss in the segment does not change with r . This is an artifact due to the imposed periodic boundary condition. Since the total number of vehicles

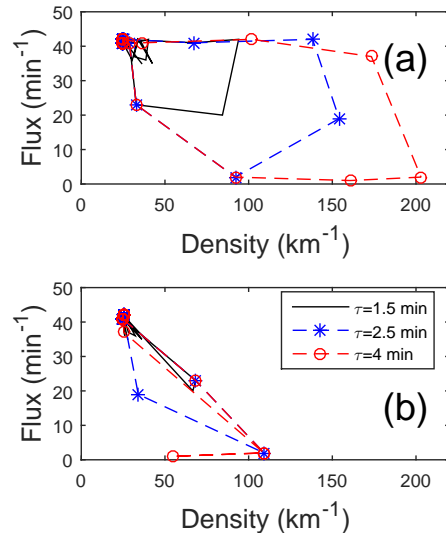


Figure 11. The evolution of the system during accident with (a) the 2-point measure, and (b) the 1-point measure. The black solid line, the blue dashed line with stars, and the red dashed line with circles correspond to different scale of accidents, $\tau = 1.5$ min, 2.5 min, and 4 min, respectively.

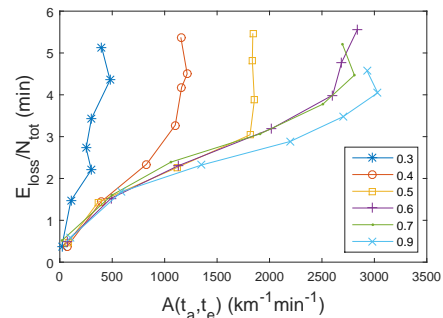


Figure 12. The economic loss per vehicles versus the area enclosed, for various accident position $x = r \|x_2 - x_1\|$ and controlling time τ . Each line corresponds to different values of r , increasing from the leftmost curve, $r = 0.3$, to the leftmost curve, $r = 0.9$. Points on the line indicates different values of τ . With a larger τ , the economic loss per vehicles is larger.

in the system is fixed, there is a maximum density in the detecting segment, with the accumulation $\alpha = N$. The maximum value of $A(t_a, t_e)$ is reached when all vehicles in the system are inside the segment during the accident. This would not happen in real traffic systems, as there are always vehicles entering the system.

The saturation for small r has a different cause. Because of the accident, vehicles are queuing up from the accident site $x = r \|x_2 - x_1\|$. If the accident site is closer to the upstream end, the maximum accumulation of the segment decreases. This results in a smaller $A(t_a, t_e)$. Assume that the back propagation speed of congestion is w , the segment reaches the maximum accumulation

if $\tau \geq \frac{r\|x_2-x_1\|}{w}$. In contrast to the saturation for large r , this is possible when an accident is so serious that the road clearing time is too long. This suggests a possibility in extracting the accident information (location and road clearing time) from the graph of $\frac{E_{\text{loss}}}{N_{\text{eff}}}$ versus $A(t_a, t_e)$ through calibration, if we have both quantities. It is possible to identify the black spot of accidents on a segment.

V. DISCUSSION AND CONCLUSION

To describe the phenomenon of congestion, we have shown that it is more reliable in using a segment-wise description. The 2-point measure is more robust to speed fluctuations during congestion, and reflects the reference density and flux in the simulation of the optimal velocity model.

Through the consideration of trajectories during congestion, we introduce the area enclosed by the trajectory as an important quantity in describing dynamics during congestion. The loss area is shown to have a physical meaning of the difference between the autocovariance of the outflux and the temporal covariance between the influx and outflux.

The loss area constructed by the 2-point measure is much more useful in the study of the congestion event than its 1-point measure counterpart, including the identification of the regimes of moderate flow and serious congestion, and its relation to the economic loss.

Although the information gathered by 1-point measure on two consecutive detectors is sufficient to obtain the observables in the 2-point measure, the 2-point measure should not be treated as a simple extension of the 1-point measure. Equation (13) shows that the loss area is a product of the congestion time interval with the covariance between the influx and outflux. The congestion time interval is defined as the interval when the accumulation or the latency across a segment is greater than some threshold values. Without the concept of segment in the 1-point measure, it can only give the covariance between the influx and outflux, but not the congestion time interval.

It is also shown that the loss area by the trajectory is proportional to the economic loss incurred by congestion. Incidentally, this is reminiscent of hysteresis curves in thermodynamics where the loss area in the space of stimulus and response represents the energy loss. With a larger loss area, the average delay incurred is also larger. This provides a way to estimate the economic loss without the knowledge of trajectories of every vehicle on the road.

By investigating the relation between the loss area and the flux fluctuation during congestion, we find that the loss area rises significantly when the flux fluctuation is greater than a threshold. This supports the existence of two dynamics during congestion. As illustrated on the fundamental diagram, one is a loopy evolution, which is

triggered by a sharp drop in flux. The other one is a random fluctuation around a moderate level of flux independence of density. These two behaviors are named as “the serious congestion” and “the moderate flow”, respectively.

These dynamics should not be treated as evidence of the three phase traffic theory by Kerner, as they are not related to the behavior at the downstream front, and much more refined space-time trajectories of individual vehicles unavailable from our data source are needed to make further assessment. It is fine to propose two states of congestion, but tracing the dynamics of the system state in the fundamental diagram provides a fuller picture of congestion than a time-averaged one.

It is obvious that the serious congestion has a greater impact to the society, compared to the moderate flow. As congestion is inevitable due to demand in peak hours, it might be possible to be focus on maintaining the moderate flow instead. Indeed, flow control by limiting the number of vehicles entering the system has been implemented in highway systems [4]. Our study will be able to quantify the costs and benefits in optimizing such measures.

ACKNOWLEDGMENTS

We thank the help from Eman Tai, Yulin Xu, and K.T. Siu in managing the data from Taiwan highway system. This work is supported by the Research Grants Council of Hong Kong (grant numbers 16322616 and 16306817).

Appendix A: The Relation of the Area Enclosed with the Temporal covariance

Following the definition of the area enclosed in Eq. (12),

$$A(t_a, t_e) = \oint \Phi_{\text{out}}(t) d\rho_2(t), \quad (\text{A1})$$

where the path of integration is taken to be within the congestion time interval $[t_a, t_e]$. When the time interval is chosen precisely, $(\rho_2(t_a), \Phi_{\text{out}}(t_a))$ is close to $(\rho_2(t_e), \Phi_{\text{out}}(t_e))$. The area enclosed is simplified as

$$A(t_a, t_e) = \int_{t_a}^{t_e} \Phi_{\text{out}}(t) \left(\frac{d}{dt} \rho_2(t) \right) dt, \quad (\text{A2})$$

From the definition of density in 2-point measure, Eq. (7), and the conservation of flow, Eq. (8),

$$A(t_a, t_e) = \frac{1}{L} \int_{t_a}^{t_e} \Phi_{\text{out}}(t) (\Phi_{\text{in}}(t) - \Phi_{\text{out}}(t)) dt. \quad (\text{A3})$$

By introducing the averaged flux $\bar{\Phi}_{\text{in}}, \bar{\Phi}_{\text{out}}$,

$$\bar{\Phi}_{\text{in}} = \frac{1}{|t_e - t_a|} \int_{t_a}^{t_e} \Phi_{\text{in}}(t) dt, \quad (\text{A4})$$

$$\bar{\Phi}_{\text{out}} = \frac{1}{|t_e - t_a|} \int_{t_a}^{t_e} \Phi_{\text{out}}(t) dt, \quad (\text{A5})$$

we consider the replacement,

$$\Phi_{\text{in}}(t) = \bar{\Phi}_{\text{in}} + \Phi_{\text{in}}(t) - \bar{\Phi}_{\text{in}}, \quad (\text{A6})$$

$$\Phi_{\text{out}}(t) = \bar{\Phi}_{\text{out}} + \Phi_{\text{out}}(t) - \bar{\Phi}_{\text{out}}, \quad (\text{A7})$$

in Eq. (A3).

$$A(t_a, t_e) = \frac{|t_e - t_a|}{L} [\bar{\Phi}_{\text{out}} \bar{\Phi}_{\text{in}} - \bar{\Phi}_{\text{out}} \bar{\Phi}_{\text{out}}] + \frac{|t_e - t_a|}{L} \times (\text{cov}_{[t_a, t_e]}(\Phi_{\text{in}}, \Phi_{\text{out}}) - \text{cov}_{[t_a, t_e]}(\Phi_{\text{out}}, \Phi_{\text{out}})), \quad (\text{A8})$$

where

$$\text{cov}_{[t_a, t_e]}(A, B) = \frac{1}{|t_e - t_a|} \times \int_{t_a}^{t_e} (A(t) - \bar{A}(t)) (B(t) - \bar{B}(t)) dt, \quad (\text{A9})$$

denotes the covariance of the two time series $A(t)$ and $B(t)$ in the time interval $[t_a, t_e]$.

During $[t_a, t_e]$, the total number of vehicles entering (exiting) the segment is $|t_e - t_a| \bar{\Phi}_{\text{in}}$ ($|t_e - t_a| \bar{\Phi}_{\text{out}}$). Since the system fully recovers from the congestion at t_e ,

$$\bar{\Phi}_{\text{in}} \approx \bar{\Phi}_{\text{out}}. \quad (\text{A10})$$

The contribution from the first term in Eq. (A8) would be negligible. The area enclosed $A(t_a, t_e)$ would be dominated by the covariance term. Hence,

$$A(t_a, t_e) \approx \frac{|t_e - t_a|}{L} \times (\text{cov}_{[t_a, t_e]}(\Phi_{\text{in}}, \Phi_{\text{out}}) - \text{cov}_{[t_a, t_e]}(\Phi_{\text{out}}, \Phi_{\text{out}})). \quad (\text{A11})$$

Appendix B: Approximate Relation between the Economic Loss and the Area Enclosed

Following the physical picture of the loopy dynamics during congestion, we consider an accident happening in the system and congestion propagates backward to the upstream end. By computing the economic loss and the area enclosed in this situation, we have an approximate relation between them.

Suppose an accident happens on a segment of length L and the segment is completely blocked at the accident site in $[t_a, t_e]$. The serious congestion consists of two major stages, the queueing of vehicles and the recovery to the free flow. We assume that the traffic conditions in the upstream and downstream segments are similar, which also agrees with our observations of the time series in the real data. Then the time taken in each stage is roughly the same, and can be approximated as $\frac{1}{2}|t_e - t_a|$. For a sufficiently long $[t_a, t_e]$, the relaxation time of congestion can be negligible, and hence, every vehicles spent

$\frac{1}{2}|t_e - t_a|$ more time on the segment. The economic loss caused by this congestion is approximated by

$$E_{\text{loss}} = \frac{1}{2} |t_e - t_a| N_{\text{tot}}, \quad (\text{B1})$$

$$N_{\text{tot}} = \int_{t_a}^{t_e} \Phi_{\text{in}}(t) dt, \quad (\text{B2})$$

with N_{tot} being the number of vehicles using the segment during congestion. We assume that the system is in a steady state before the accident happens, and hence the flux is uniform over the whole segment, i.e. $\Phi_{\text{out}} \approx \Phi_{\text{in}} = \Phi_{\text{acc}}$, where Φ_{acc} denotes the flux over the whole system just before the accident. During this congestion, the system will evolve through an anticlockwise loop on the fundamental diagram. The outflux drop from Φ_{acc} to 0 by assumption.

$$\Delta\Phi_{\text{out}} = -\Phi_{\text{acc}}. \quad (\text{B3})$$

The accumulation grows according to the number of vehicles entering the system during the time interval,

$$\Delta\alpha \approx \Phi_{\text{acc}} |t_e - t_a|. \quad (\text{B4})$$

Here, it is assumed that the accident in the segment does not affect the influx, and the segment upstream of the accident site is not yet fully occupied during $[t_a, t_e]$. The area enclosed during this accident would be

$$A(t_a, t_e) \approx |\Delta\Phi_{\text{out}}| \times \frac{\Delta\alpha}{L} = \frac{\Phi_{\text{acc}}^2}{L} |t_e - t_a|. \quad (\text{B5})$$

$$\frac{E_{\text{loss}}}{N_{\text{tot}}} \approx \frac{L}{2\Phi_{\text{acc}}^2} A(t_a, t_e). \quad (\text{B6})$$

If we consider the general case that the segment is only partially blocked by the accident, then the outflux Φ_{out} drop by a fraction $(1-f)$ to $(1-f)\Phi_{\text{acc}}$. Φ_{acc} in Eqs. (B3) to (B5) should be replaced by $f\Phi_{\text{acc}}$. On the other hand, it is noted that under this condition, not all vehicles are delayed by $\frac{1}{2}|t_e - t_a|$. We simplify the situation by assuming that the vehicles are noninteracting; one possible scenario for a multi-lane highway is that vehicles along some lanes are blocked by accidents and are unable to switch lanes while those along other lanes can travel at normal speed. We then arrive at an effective model in which vehicles are separated into two classes, the affected vehicles and the unaffected vehicles. The number of affected vehicles can be approximated by fN_{tot} . There is negligible delay for the unaffected vehicles, and hence the economic loss per vehicle should be

$$\frac{E_{\text{loss}}}{N_{\text{tot}}} \approx \frac{1}{N_{\text{tot}}} \left(fN_{\text{tot}} \left(\frac{1}{2} |t_e - t_a| \right) + (1-f)N_{\text{tot}} \times 0 \right), \quad (\text{B7})$$

$$\frac{E_{\text{loss}}}{N_{\text{tot}}} \approx \frac{L}{2f\Phi_{\text{acc}}^2} A(t_a, t_e). \quad (\text{B8})$$

In fact, Φ_{acc} is bounded above by the maximum flux at free flow, Φ_{max} due the physical limit of road capacity. Hence the area enclosed could give an approximation of the lower bound of the averaged economic loss $\frac{E_{\text{loss}}}{N_{\text{tot}}}$.

$$\frac{E_{\text{loss}}}{N_{\text{tot}}} \gtrsim \frac{L}{2f\Phi_{\text{max}}^2} A(t_a, t_e). \quad (\text{B9})$$

It is possible to approximate the number of affected ve-

hicles N_{tot} by its lower bound, which is the number of vehicles coming in during congestion, $\Phi |t_e - t_a|$. The lower bound of the total economic loss E_{loss} would be given by

$$E_{\text{loss}} \gtrsim \frac{L}{2f\Phi_{\text{max}}} |t_e - t_a| A(t_a, t_e). \quad (\text{B10})$$

-
- [1] Richard Cole, Yevgeniy Dodis, and Tim Roughgarden. Pricing network edges for heterogeneous selfish users. In *Proceedings of the thirty-fifth annual ACM symposium on Theory of computing*, pages 521–530. ACM, 2003.
- [2] Robert B Cooper. *Introduction to queueing theory*. North Holland,, 1981.
- [3] Carlos F Daganzo. Requiem for second-order fluid approximations of traffic flow. *Transportation Research Part B: Methodological*, 29(4):277–286, 1995.
- [4] Carlos F Daganzo. Urban gridlock: Macroscopic modeling and mitigation approaches. *Transportation Research Part B: Methodological*, 41(1):49–62, 2007.
- [5] LC Davis. Driver choice compared to controlled diversion for a freeway double on-ramp in the framework of three-phase traffic theory. *Physica A: Statistical Mechanics and its Applications*, 387(25):6395–6410, 2008.
- [6] Leslie C Edie. *Highway capacity manual*. Port of New York Authority, 1963.
- [7] Kun Gao, Rui Jiang, Shou-Xin Hu, Bing-Hong Wang, and Qing-Song Wu. Cellular-automaton model with velocity adaptation in the framework of kerner three-phase traffic theory. *Physical Review E*, 76(2):026105, 2007.
- [8] Nikolas Geroliminis, Carlos F Daganzo, et al. Macroscopic modeling of traffic in cities. In *TRB 86th annual meeting*, number 07-0413, 2007.
- [9] Arvind Kumar Gupta and Isha Dhiman. Phase diagram of a continuum traffic flow model with a static bottleneck. *Nonlinear Dynamics*, 79(1):663–671, 2015.
- [10] Serge P Hoogendoorn, Hans van Lint, and Victor L Knoop. Macroscopic modeling framework unifying kinematic wave modeling and three-phase traffic theory. *Transportation Research Record*, 2088(1):102–108, 2008.
- [11] Bin Jia, Xin-Gang Li, Tao Chen, Rui Jiang, and Zi-You Gao. Cellular automaton model with time gap dependent randomisation under kerner three phase traffic theory. *Transportmetrica*, 7(2):127–140, 2011.
- [12] Cheng-Jie Jin, Wei Wang, Rui Jiang, HM Zhang, and Hao Wang. Spontaneous phase transition from free flow to synchronized flow in traffic on a single-lane highway. *Physical Review E*, 87(1):012815, 2013.
- [13] Boris Kerner. Congested traffic flow: Observations and theory. *Transportation Research Record: Journal of the Transportation Research Board*, (1678):160–167, 1999.
- [14] Boris S Kerner. Experimental features of self-organization in traffic flow. *Physical review letters*, 81(17):3797, 1998.
- [15] Boris S Kerner. The physics of traffic. *Physics World*, 12(8):25, 1999.
- [16] Boris S Kerner. The physics of traffic: empirical freeway pattern features, engineering applications, and theory. *Physics Today*, 58(11):54–56, 2005.
- [17] Boris S Kerner. Failure of classical traffic flow theories: stochastic highway capacity and automatic driving. *Physica A: Statistical Mechanics and its Applications*, 450:700–747, 2016.
- [18] Boris S Kerner and Hubert Rehborn. Experimental properties of complexity in traffic flow. *Physical Review E*, 53(5):R4275, 1996.
- [19] Boris S Kerner, Sergey L Klenov, and Michael Schreckenberg. Probabilistic physical characteristics of phase transitions at highway bottlenecks: incommensurability of three-phase and two-phase traffic-flow theories. *Physical Review E*, 89(5):052807, 2014.
- [20] BS Kerner. Synchronized flow as a new traffic phase and related problems for traffic flow modelling. *Mathematical and Computer Modelling*, 35(5-6):481–508, 2002.
- [21] Michael James Lighthill and Gerald Beresford Whitham. On kinematic waves ii. a theory of traffic flow on long crowded roads. *Proc. R. Soc. Lond. A*, 229(1178):317–345, 1955.
- [22] Daniel V McGehee, Elizabeth N Mazzae, and GH Scott Baldwin. Driver reaction time in crash avoidance research: validation of a driving simulator study on a test track. In *Proceedings of the human factors and ergonomics society annual meeting*, volume 44, pages 3–320. SAGE Publications Sage CA: Los Angeles, CA, 2000.
- [23] Kai Nagel and Michael Schreckenberg. A cellular automaton model for freeway traffic. *Journal de physique I*, 2(12):2221–2229, 1992.
- [24] Kai Nagel, Peter Wagner, and Richard Woesler. Still flowing: Approaches to traffic flow and traffic jam modeling. *Operations research*, 51(5):681–710, 2003.
- [25] Kai Nagelocd and Steen Rasmussenaf. Traffic at the edge of chaos. In *Artificial Life IV: Proceedings of the Fourth International Workshop on the Synthesis and Simulation of Living Systems*, volume 4, page 222. MIT Press, 1994.
- [26] Gordon F Newell. A simplified theory of kinematic waves in highway traffic, part i: General theory. *Transportation Research Part B: Methodological*, 27(4):281–287, 1993.
- [27] Daiheng Ni, John D Leonard, and Marston Hall. Direct methods of determining traffic stream characteristics by definition. *Transportation Research Record*, 2004.
- [28] Gábor Orosz, R Eddie Wilson, Róbert Szalai, and Gábor Stépán. Exciting traffic jams: nonlinear phenomena behind traffic jam formation on highways. *Physical review E*, 80(4):046205, 2009.
- [29] Gábor Orosz, R Eddie Wilson, and Gábor Stépán. Traffic jams: dynamics and control, 2010.
- [30] Paul I Richards. Shock waves on the highway. *Operations*

- research*, 4(1):42–51, 1956.
- [31] Martin Schönhof and Dirk Helbing. Empirical features of congested traffic states and their implications for traffic modeling. *Transportation Science*, 41(2):135–166, 2007.
- [32] Martin Schönhof and Dirk Helbing. Criticism of three-phase traffic theory. *Transportation Research Part B: Methodological*, 43(7):784–797, 2009.
- [33] Yūki Sugiyama. Optimal velocity model for traffic flow. *Computer Physics Communications*, 121:399–401, 1999.
- [34] Yuki Sugiyama, Minoru Fukui, Macoto Kikuchi, Katsuya Hasebe, Akihiro Nakayama, Katsuhiko Nishinari, Shin-ichi Tadaki, and Satoshi Yukawa. Traffic jams without bottlenecks - experimental evidence for the physical mechanism of the formation of a jam. *New journal of physics*, 10(3):033001, 2008.
- [35] D Washington. Highway capacity manual. *Special Report*, 209, 1985.
- [36] Gerald Beresford Whitham. *Linear and nonlinear waves*, volume 42. John Wiley & Sons, 2011.
- [37] Hai Yang and Xiaolei Wang. Managing network mobility with tradable credits. *Transportation Research Part B: Methodological*, 45(3):580–594, 2011.